NEW METHODS FOR INSPECTION AND EVALUATION OF STEEL GUSSET PLATE CONNECTIONS

Christopher Higgins[1] and O. Tugrul Turan[2]

Abstract

A new methodology was developed to collect accurate field measurements to support structural evaluations of steel truss bridge gusset plate connections. The method uses close-range photogrammetry to rectify field-collected digital images to produce scaled orthographic photographs (orthophotos) of bridge connections. Using the orthophotos, true-scale geometric measurements are made of the plate and fasteners. The geometric data can be compared with design and fabrication drawings and used to assess connection capacity. The methods and models have been deployed in the field and are finding broad acceptance.

Introduction and Background

Evaluation of gusset plate connections has become important for many transportation agencies in the US due to the recent collapse of the I-35W Bridge in Minnesota. According to the Federal Highway Administration, there are approximately 465 steel deck truss bridges within the National Bridge Inventory (NTSB Recommendations 2008). Even larger numbers of other types of steel truss bridges (approximately 12,600) exist in the inventory. Many of these bridges are undergoing additional scrutiny because the load paths are non-redundant, thus failure in a truss member or connection may cause the structure to collapse. Connection evaluations require complete and accurate as-built drawing sets and condition reports. Most connection evaluations use design drawings and traditional design methods to conduct ratings. Current methods to measure, collect, and archive field data are time consuming as illustrated in Fig. 1 and subject to errors at all stages. Additionally, field data will need to be archived to monitor and evaluate changes over the life of the structure. Sketches, notes, and qualitative photographic images may not be sufficient to provide definitive answers to time-dependent changes.

Tools that can effectively capture field data to provide analysis inputs will hasten the complex and time consuming task of steel truss bridge connection evaluation. This paper reports on research that developed methods to create orthographic digital

[1] Professor, School of Civil and Construction Engineering, Oregon State University, Corvallis, OR

[2] Assistant Professor, Dept. of Civil Engineering, Istanbul Technical University, Istanbul, Turkey

photographs (orthophotos) that enable metrification of steel truss bridge gusset plate connections. Data extraction from the images is ported directly to scripted Finite Element Analyses (FEA) to determine connection ratings. These combined techniques enable rapid and accurate quantitative field geometry acquisition and evaluation of connections. Integration of field data collection and analysis tasks further streamlines bridge management efforts.

FIGURE 1 – EXAMPLE OF STATE-OF-THE-PRACTICE METHOD USED TO COLLECT FIELD DATA ON GUSSET PLATE CONNECTION GEOMETRY

Visual inspection methods are now beginning to deploy supporting technologies that can improve and accelerate structural evaluations (McCrea et al. 2002). One type of technology is digital image processing, which has been utilized in various civil engineering fields. Several researchers implemented digital image technologies for assessment and inspection of steel, concrete and reinforced concrete structures. Although using digital image processing to detect a crack on a concrete surface is difficult due to voids, blemishes, shading, and shapes of cracks, it has attracted broad interest and been studied by several researches such as Ito *et al*. (2002), Dare *et al*. (2002), Hutchinson and Chen (2006), Fujita *et al*. (2006), Yamaguchi and Hashimoto (2006),Yamaguchi *et al*. (2008), and Yamaguchi and Hashimoto (2009). Lee and Chang (2005) used digital image processing for the assessment of rust defects on steel bridges. Liu et al. (2006) utilized image processing methods to detect rivets for aircraft lap joints. Simple and effective close-range photogrammetry techniques have been utilized in historical building documentation (Arias *et al*., 2007) and several researchers have used close-range photogrammetry for metrification such as Heuvel (1998), Criminisi *et al*. (2000), Tommaselli *et al*. (2005), Rodriguez *et al*. (2008). In this paper digital image processing is used to rectify digital photographs to produce scaled orthographic images (orthophotos) of steel truss bridge gusset plate connections so that physical dimensions can be extracted and used in

connection evaluation. The present study differs from previous work because for evaluation of truss bridges, photographs cannot easily be taken from a mounted stationary position. In the field, photographs of bridge gusset plates will likely be taken from a snooper with both the snooper and bridge in motion from wind and traffic, or by climbing on the structure, and thus it will not be feasible to obtain stationary positions to correlate stereo or multi-station images.

Image Rectification and Metrification with Flat-Field Lenses

Photographs are taken of a real world image and placed on a two-dimensional image plane. When an image is captured with a camera and lens, it generally contains perspective distortion (parallel lines converging at a finite point), as well as other distortions due to the lens characteristics (such as barrel distortion or pin-cushion). To remove perspective, the image can be rectified using a mathematical transformation which maps elements in the real world image to those in the photographic image plane. To remove barrel distortion or pin-cushion, either flat field lenses must be deployed or lens correction parameters can be used to post-process images.

For the present case, barrel distortion and pin-cushion are minimized by using lenses that minimize these distortions. When the salient features of the real world image correspond generally to a single plane, as is the present case for gusset plate connections, two-dimensional correspondences can be used to rectify the image, which simplifies the transformation. One of the most common techniques for image rectification is the direct linear transformation (DLT) algorithm. This transformation requires that certain geometrical characteristics be established between in the real world image and the image plane so that the image can be rectified. In the present case, point correspondences are used to map points between the real world image and the photographic image plane based on central projection shown in Fig. 2. Central projection maps the common points between planes and preserves lines in both planes.

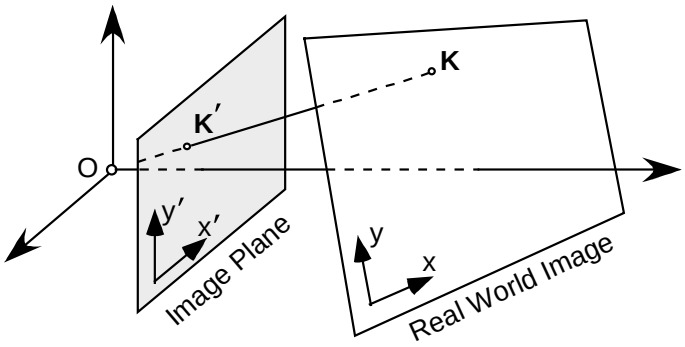

FIGURE 2 – CORRESPONDENCES BETWEEN PHOTOGRAPHIC IMAGE PLANE AND REAL WORLD IMAGE

When the geometrical features are established so as to provide a true dimensional scale, the resulting transformation is not only rectified, it is scaled to the real world dimensions. This allows metrification from the rectified image. For implementation of the DLT algorithm, the image plane and real world planes are assumed to be homogeneous. A transformation matrix, H, is determined to satisfy the following equation for each control point, i:

$$H\begin{bmatrix} X_i' \\ Y_i' \\ 1 \end{bmatrix} = \begin{bmatrix} X_i \\ Y_i \\ 1 \end{bmatrix} \tag{1}$$

where X' and Y' are photograph image plane control point coordinates, X and Y are real world control point coordinates, and H is a 3x3 matrix. To solve for the transformation matrix H, a minimum of four control points are needed (x and y coordinates each provide a degree-of freedom (DOF) for a total of eight DOFs and one more is provided by scale, thereby providing nine DOFs to solve for the matrix). If more points are available, error estimations can be made. The method generates a two-dimensional transformation based solely on the control point coordinates, thus, camera parameters are not needed. Such DLT algorithms are used in commercial photogrammetric software.

Implementation of the DLT requires that known control points be established in the real world image that can be captured in the image plane. For the present research, reference targets were developed that are placed on a gusset plate. These targets establish nine (9) control points which provide more image constraints than the minimum required to solve for the transformation matrix, thereby enabling error estimation. The control points are spread throughout the image. The reference target control points standoff from the surface of the gusset plate, which is necessary for clearance over bolt and rivet heads, but this standoff distance causes the reference target to appear larger in the photograph than if it were to lie explicitly on the gusset plate surface. The offset can be corrected assuming the camera is a single point and using similar triangles to calculate the apparent size increase of the reference target compared to if it were to lie on the gusset plate surface. The standoff distance for the reference targets used in this study is approximately 51 mm (2 in.) from the gusset plate surface. The actual lengths of the gusset plate features including the offset correction can be calculated as:

$$L_{actual} = \frac{D}{D - D_o} L_{image} \tag{2}$$

where D is the distance from the camera to the gusset plate surface, D_o is the target standoff distance, and L_{image} is the uncorrected length measured in the image. Dimensions taken from the rectified image without standoff correction will be smaller than the true dimensions. If the camera location if very far away from the target, the correction becomes small (e.g. correction is less than 5% for camera located 1.5 m (5 ft) from the gusset plate).

To rapidly establish repeatable control points in the real world image, two reference targets were developed. One is relatively small with 203 mm (8 in.) arms and the other is relatively large with 610 mm (24 in.) arms. The small reference target is used for smaller gusset plates or for splice plates between chord members. The large reference target is used for most typical large gusset plate connections. The targets use 12.7 mm (0.5 in.) square Ultra Corrosion-Resistant Pure Titanium Grade 2 bars, nine (9) aluminum discs that serve as the control points, and an aluminum encased round ceramic magnet. The nine aluminum discs are equally spaced along the titanium bars. The aluminum cylinder base is bolted along with the ceramic magnet to the center of the bars. The magnetic base allows the reference target to be held securely on the gusset plate surface, even with many layers of paint, to be easily reused, and to leave the gusset plate undamaged. The reference target shown on a large gusset plate is shown in Fig. 3.

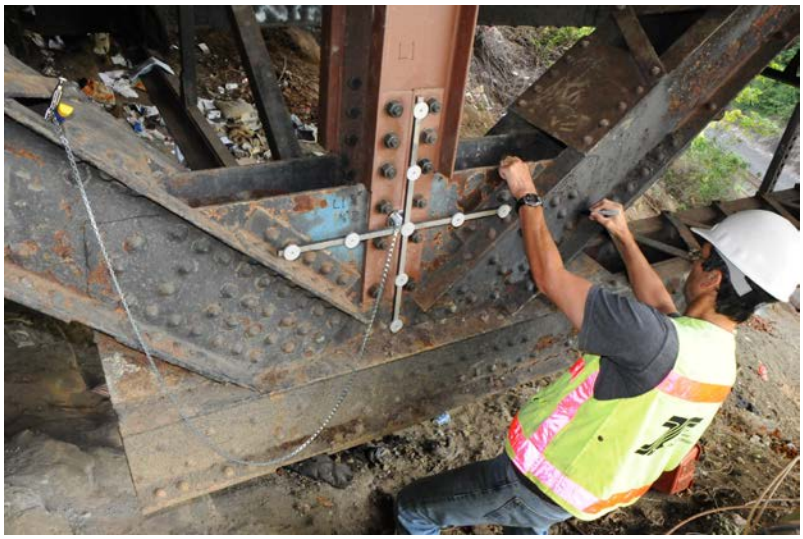

FIGURE 3 - REFERENCE TARGET ON GUSSET PLATE USED TO ESTABLISH CONTROL POINTS IN REAL WORLD IMAGE

The image rectification and metrification process was written using MATLAB (The Mathworks, 2010) and deploys the Image Processing Toolbox within MATLAB. A digital image of a gusset plate with the reference target is taken. The gusset plate digital photograph is loaded into the program and the image pixels of the reference targets are selected by the user. These establish the known real world target coordinates for the DLT algorithm. As part of the processing, an origin is established at the center of the target. The rectified image is presented to the user for validation and then stored for future reference. After processing, the user can query the image to extract geometric data of interest, because the methodology has converted the pixel size to a true-scale dimension (for example - mm).

To illustrate the methodology and find the difference between measured and the computer numerical control machine (CNC) fabricated gusset plate dimensions, a full size

CNC fabricated gusset plate was used. Images were captured with a digital single-lens reflex (SLR) camera made by Nikon (Nikon D300s). The camera uses a 12.3 Megapixel (4288 x 2848) CMOS sensor. The lens was an autofocus fixed 60 mm f2.8D lens. The non-metric digital camera was not calibrated. Field inspectors will likely be using a variety of digital cameras with various lenses and zoom capability and these cameras will not be mounted on a tripod or stationary platform while images are taken. Controlled calibration may not be feasible or transferable to field applications and thus, cameras and the techniques deployed must be compatible with hand-held operation under realistic field conditions. To reflect these conditions, the images were taken in the laboratory under realistic imaging conditions. Three images; 90 degrees between the gusset plate surface and the normal of the image plane (S90), 30 degrees between the gusset plate surface and the normal of the image plane from the left (S30L), 30 degrees between the gusset plate surface and the normal of the image plane from right (S30R), were taken. The original and rectified images are shown in Fig. 4. Qualitative comparison of the collected geometry of the gusset plate and the original geometry are shown in Fig.5.

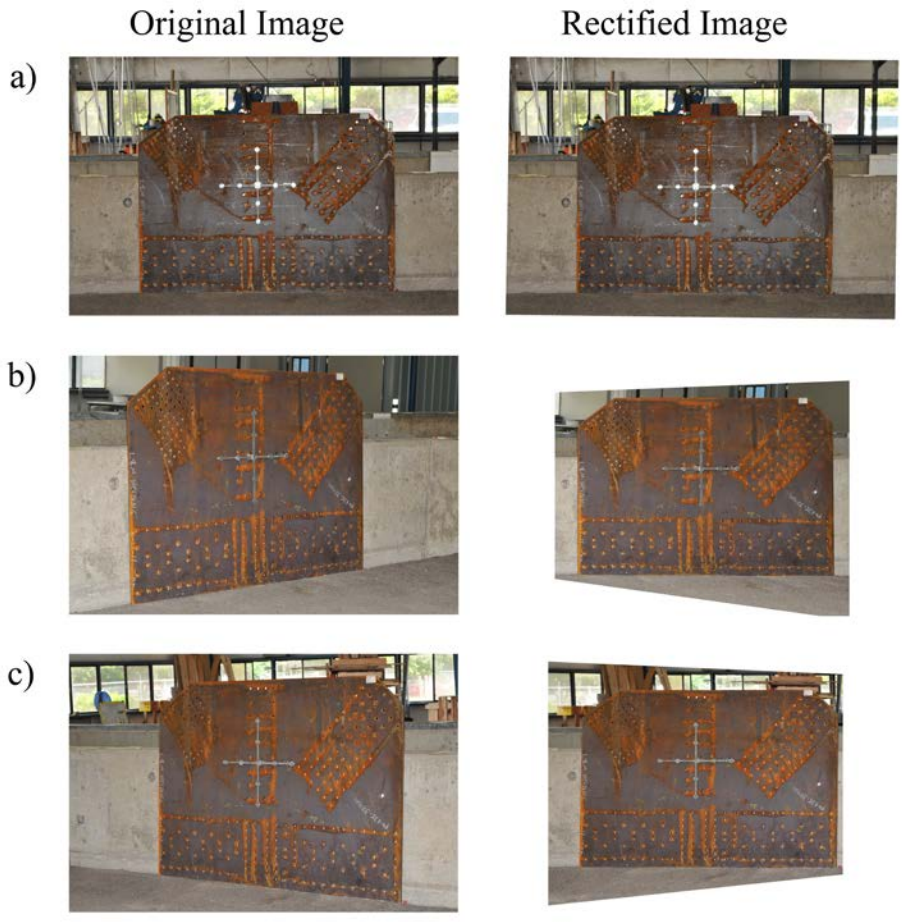

FIGURE 4 – ORIGINAL AND RECTIFIED IMAGES A) S90, B) S30L, AND C) S30R

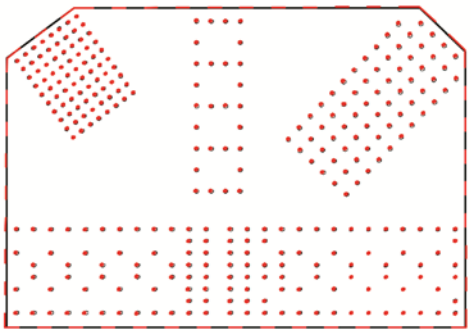

FIGURE 5 – EXAMPLE OF EXPECTED (BLACK) AND MEASURED (RED) PLATE AND FASTENER LOCATIONS (CASE S90 SHOWN).

In order to conduct a quantitative comparison with respect to the present application to gusset plate evaluation, the procedures in the FHWA Load Rating Guidance and Examples for Bolted and Riveted Gusset Plates in Truss Bridges (FHWA, 2009) were used. To perform evaluations of the various connection failure modes, input geometries are needed. Geometric measures for the following modes were used: gross length along the plane resisting tension stress Bl. Sh. (T) and gross length along the plane resisting shear stress (Bl. Sh. (V)) for block shear evaluation of every member in the gusset plate, unbraced buckling length (Buc. Len.) and Whitmore Width (W. Width) and for every compression member, gross length of the plate resisting horizontal shear (H. Sh.), gross length of the plate resisting vertical shear (H. Sh.) and edge lengths (A, B, C, D, E, F) were measured as shown in Fig. 6. A histogram showing the percent difference across all the structural dimensions for case S90 are shown in Fig. 7. The absolute value of the observed maximum differences were 0.92%, 1.91% and 1.86%; and the mean differences were -0.07%, 0.12% and 0.18% for S90, S30L and S30R, respectively. As expected, the image with the least amount of initial perspective, S90, produced slightly better results. However, even the other two images with strong perspective provided quite good outcomes that are well within the expected needs of bridge engineers performing connection evaluations.

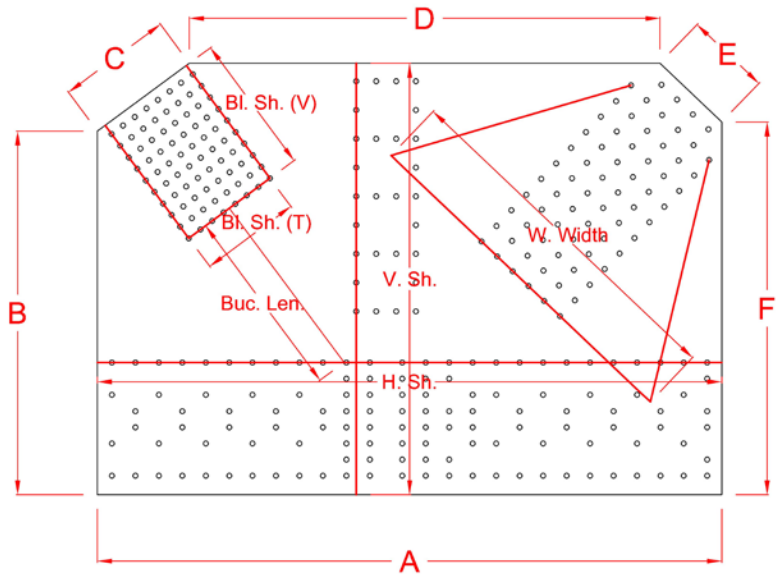

FIGURE 6 - GUSSET PLATE GEOMETRIC PARAMETERS USED TO COMPARE THE IMAGE MEASUREMENT WITH THE CNC INPUT FILE GEOMETRY (FOR SIMPLICITY BL. SH. (V), BL. SH. (T), BUC. LEN, W. WIDTH ARE NOT SHOWN FOR EVERY MEMBER).

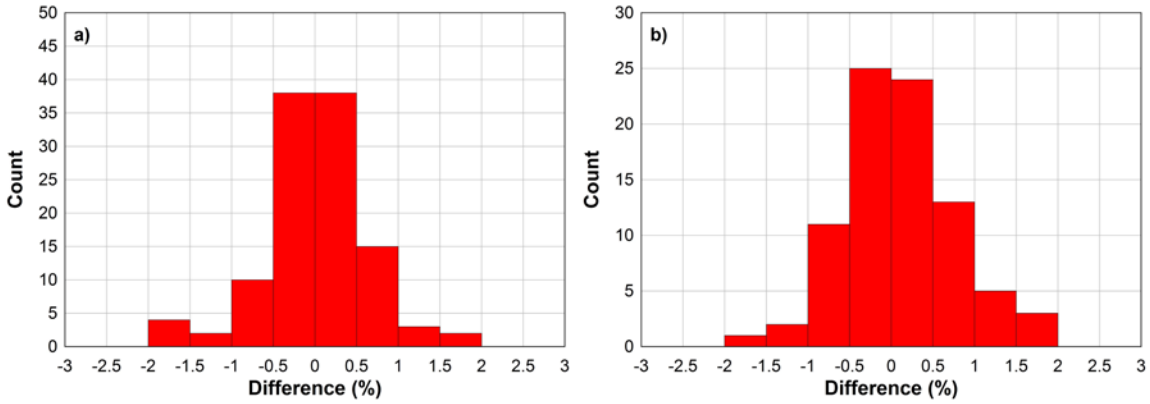

FIGURE 7 - HISTOGRAM OF DIFFERENCES BETWEEN EXPECTED AND MEASURED VALUES FOR STRUCTURAL EVALUATION PARAMETERS FROM A) FLAT-FIELD LENS B) FISHEYE LENS.

Image Rectification and Metrification with Fisheye Lenses

Flat-field lenses were used in the previous development in order to minimize the effect of barrel distortion and/or pin-cushion. However, due to the size and short available standoff distance, it is sometimes difficult to capture the whole gusset plate in one picture with a short focal length lens. Furthermore, sometimes due to obstacles such as another gusset plate, floor beam, lateral bracing, utility pipe etc., it is impossible to capture the whole gusset plate in one picture with a flat-field lens. For these cases, a fisheye lens can

be utilized to capture a large part of the structure with short focal lengths. A fisheye image can then be converted to a perspective image (defish) so that the converted image (defished image) can be used in rectification and metrification procedures as described above.

Fisheye lenses are lenses that can provide a wide field of view with a very short focal length. These lenses can be used to capture 180^{o} or larger field of view with a single camera, from one stationary point and at a single moment (Abraham and Forstner, 2005). Compared to a true panoramic camera, they are inexpensive and can be combined with conventional cameras (Scheneider *et al*., 2009).

In fisheye projection models, generally a sphere is projected on a plane and depending on their projection geometry; they can be classified in four different categories: Equidistant Projection, Equisolid-angle Projection, Othographic Projection and Stereographic Projection (Ray, 1994). Most of fisheye lenses are either Equisolid-angle Projection or Equidistant Projection. In this paper Equisolid-angle Projection was used for defishing images.

In perspective projection, an object in space can be described in the camera coordinate system as and the same object can be described in the image coordinate system as where and axes and and axes are parallel. Using this notation, the incidence angle, image radius, and the mapping function of an undistorted perspective image can be written (Scheneider *et al*., 2009) as:

$$\tan(\alpha) = \frac{\sqrt{x^2 + y^2}}{z} \tag{1}$$

$$r' = \sqrt{x'^2 + y'^2} \tag{2}$$

$$r' = c_1 \tan(\alpha) \tag{3}$$

$$\frac{x_1'}{y_1'} = \frac{x}{y} \tag{4}$$

where c_1 is the principle distance of the undistorted perspective image. Using Eqs.5-6 (x_1', y_1') can be written as:

$$x_1' = \frac{r'}{\sqrt{\left(\frac{y}{x}\right)^2 + 1}}$$
$$y_1' = \frac{r'}{\sqrt{\left(\frac{x}{y}\right)^2 + 1}} \tag{5}$$

Utilizing Eq.3, 5; (x_1', y_1') can also be written as:

$$x_1^{'} = \frac{c_1 \frac{\sqrt{x^2 + y^2}}{z}}{\sqrt{\left(\frac{y}{x}\right)^2 + 1}}$$
$$y_1^{'} = \frac{c_1 \frac{\sqrt{x^2 + y^2}}{z}}{\sqrt{\left(\frac{x}{y}\right)^2 + 1}} \quad (6)$$

For the undistorted fisheye projection models, the mapping functions and the projection equation for Equisolid-angle Projection can be written (with correction parameters ignored) (Scheneider *et al*, 2009) as:

$$r' = 2c_2 \sin\left(\frac{\alpha}{2}\right) \quad (7)$$

$$x_2^{'} = 2c_2 \frac{\sin\left(\frac{1}{2}\arctan\left(\frac{\sqrt{x^2 + y^2}}{z}\right)\right)}{\sqrt{\left(\frac{y}{x}\right)^2 + 1}}$$
$$y_2^{'} = 2c_2 \frac{\sin\left(\frac{1}{2}\arctan\left(\frac{\sqrt{x^2 + y^2}}{z}\right)\right)}{\sqrt{\left(\frac{x}{y}\right)^2 + 1}} \quad (8)$$

In order to convert fisheye images to perspective images, fisheye images are assumed to be undistorted (correction parameters are ignored). For Equisolid-angle Projection, the perspective image coordinates were derived for the fisheye projection equations by mapping to the real world image coordinates using Eqs. 8-10 as:

$$x_1^{'} = c_1 \frac{\tan(2\sin^{-1}(\frac{x_2^{'}}{2c_2}\sqrt{\left(\frac{y_2^{'}}{x_2^{'}}\right)^2+1}))}{\sqrt{\left(\frac{y_2^{'}}{x_2^{'}}\right)^2+1}}$$
$$y_1^{'} = c_1 \frac{\tan(2\sin^{-1}(\frac{y_2^{'}}{2c_2}\sqrt{\left(\frac{x_2^{'}}{y_2^{'}}\right)^2+1}))}{\sqrt{\left(\frac{x_2^{'}}{y_2^{'}}\right)^2+1}} \quad (9)$$

Using Eq. 11, a Matlab image processing program was written. Three images; 61 cm (2 ft) away from the gusset plate (F2ft), 91 cm (3 ft) away from the gusset plate (F3ft), and 152.4 cm (5 ft) away from the gusset plate (F5ft); were taken with a Nikkor 10.5 mm lens which uses Equisolid-angle Projection. The principle distance in the x (c_{2X}) and y (c_{2Y}) directions are calculated as 1918.70 pixels (the maximum resolution in the x direction (4288) divided by the sensor size in the x direction (23.6 mm) and multiplied by the focal length (10.56 mm)) and 1903.44 pixels (the maximum resolution in the y direction (2848) is divided by the sensor size in the y direction (15.8 mm) and multiplied by the focal length (10.56 mm)). The principle distance of the perspective image (c_1) was 600 pixels which provided a large field of view from the fisheye images used in this paper. Larger values would produce a smaller portion of the image but with larger numbers of pixels across the image. The value can be selected interactively to focus on the essential part of the image and disregard superfluous portions.

The program first creates an array with the same size of the input image (fisheye image) with zeros (black) placed into the three channels (RGB (red, green, and blue). For every pixel location in the defished image, using Eq. 11 and the principle distances; the corresponding pixel location in the fisheye image was calculated. The RGB values in the fisheye image location were copied to the defished image location. If the defished image location was out of the fisheye image index, then that pixel was left blank (black). Thus, for every defished image location pixel values, the fisheye image location pixel values are copied and the defished image is created. Results are shown in Fig. 8.

Using the geometric parameters and the rectification technique described above, a quantitative comparison was conducted for each of the structural evaluation parameters described in the earlier section. Since the pictures are taken with fisheye lenses, standoff correction was not used in the metrification. Measured distances were marked on the gusset plate surface and these distances were used as a scale for metrification. The observed maximum difference was 1.11%; and the observed mean difference was 0.11%. Using all

the fisheye image measurements of the structural dimensions, a histogram was created and is shown in Fig. 7. The standard deviation was 0.67%, skewness was 0.33%, the mean was 0.12% , and there was a 99% probability that an image measurement was within +/- 1.7% of the actual. These results were comparable to the flat-field lens demonstrated previously.

FIGURE 8 - ORIGINAL, DEFISHED, AND RECTIFIED IMAGES

Conclusions

An innovative methodology that enables rectification and metrification of digital images of steel truss gusset plate connections was developed. Three programs were developed that enable an operator to quickly extract dimensional information from the scaled rectified images. Flat and fisheye lenses were used and compared with the original dimensions of a large field-scale gusset plate. The largest of the absolute maximum and mean differences between the measured and expected dimensions were 1.91% and 0.21% respectively. Dimensional measurements taken from the processed images provided results that are as good as or better than conventional field measurements and provide tolerances well below what most engineers would accept for gusset plate connection capacity calculations. Compared to traditional methods, the current method enables much more rapid, accurate, and repeatable collection of field geometric measurements. The availability of rectified pictures with metric information provides a useful record of field conditions that can be referenced in the future and compared with subsequent field inspection results to help identify and quantify long term changes in visual characteristics. These images enable comparison between available drawing sets and as-built details. Furthermore, they are being used to develop input geometries for finite element analyses of gusset plates. The implementation procedure is straightforward and does not require specialized knowledge of photogrammetry, image processing, or computer programming. It has been practically employed under field conditions using current technology and personnel. The implementation has produced significant cost savings compared to alternative methods.

Acknowledgments

This research was funded by the Oregon Department of Transportation. The input and support of Messrs. Bert Hartman, Jonathan Rooper, Jeff Swanstrom, Richard Groff, and Steven Soltesz was greatly appreciated. Mr. Quang Nguyen and Mr. Jason Killian of

Oregon State University provided assistance during early development of the image processing algorithms. The findings, conclusions, and recommendations presented are those of the authors and do not necessarily reflect the views of the project sponsors or individuals acknowledged.

References

Abraham, S., and W. Forstner, (2005). “Fish-eye-stereo calibration and epipolar rectification” ISPRS Journal of Photogrammetry and Remote Sensing, v. 59, n. 5, 278-288.

Arias, P., C. Ordóñez, H. Lorenzo, J. Herraez, and J. Armesto., (2007). “Low-cost documentation of traditional agro-industrial buildings by close-range photogrammetry”, Building and Environment, 42: 1817-1827.

Criminisi, A., I. Reid, and A. Zisserman., (2000). “Single view metrology”, Int. J. of Comp. Vision, 40: 123-148.

Dare, P. M., Hanley, H. B., Fraser, C. S., Riedel, B., and W. Niemeier, (2002). “An operational application of automatic feature extraction: the measurement of cracks in concrete structures”, The Photogrammetric Record, 17 (99), 453-464.

FHWA (2009). Load rating guidance and examples for bolted and riveted gusset plates in truss bridges” Publication No. FHWA-IF-09-014, Federal Highway Administration.

Fujita, Y., Mitane, Y., and Y. Hamamoto, (2006). “A method for crack detection on a concrete structure”, The 18th International Conference on Pattern Recognition.

Heuvel, F., (1998). “3D reconstruction from a single image using geometric constraints”, ISPRS J. of Photogrammetry and Remote Sensing, 53: 354-368. (1998).

Hutchinson, T. C., and Z. Chen, (2006). “Improved image analysis for evaluation concrete damage”, Journal of Computing in Civil Engineering 20 (3), 210-216.

Ito, A., Aoki, Y., and S. Hashimoto, (2002). “ Accurate extraction and measurement of fine cracks from concrete block surface image.” 3, 2202-2207.

Lee, S., and L. Chang, (2005). “Digital image processing methods for assessing bridge painting rust defects and their limitations.”ASCE International Conference on Computing in Civil Engineering.

Liu, Z., Forsyth, D. S., Marincak, A., and P. Vesley, (2006). “ Automated rivet detection in the EOL image for aircraft lap joints inspection.” NDT&E Intl., 39, 441-448.

Matlab 7.11.0 (R2010b), (2010). The MathWorks, Inc., Natick, MA.

McCrea, A., Chamberlain, D., and R. Navon, (2002). “Automated inspection and restoration of steel bridges-a critical review of methods and enabling technologies.” Automation in Construction, 11 (4), 351-373.

National Transportation Safety Board (NTSB) (2008). Data report state-by-state bridge counts.

Ray, S. F., (2002). “Applied photographic optics: lenses and optical systems for photography, film, video, electronic and digital imaging, Third Edition, Focal Press.

Rodríguez, J., M.T. Martín, P. Arias, C. Ordóñez, and J. Herráez. (2008) “Flat elements on buildings using close-range photogrammetry and laser distance measurement”, Optics and Lasers in Engineering, 46: 541-545.

Schneider, D., Schwalbe, E., and H. G. Maas, (2009). “Validation of geometric models for fisheye lenses” ISPRS Journal of Photogrammetry and Remote Sensing, v. 64, n. 3, 259-266

Tommaselli, A. and M. Reiss, (2005). “A photogrammetric method for single image orientation and measurement, Photogrammetric Engineering and Remote Sensing”, 71(6): 727-732.

Yamaguchi T., and S. Hashimoto, (2006). “Automated crack detection for concrete surface image using percolation model and edge information” Proceedings of the 32nd Annual Conference of the IEEE Industrial Electronics Society.

Yamaguchi, T., Nakamura, S., and S. Hashimoto, (2008). “An efficient crack detection method using percolation-based image processing.” Proceedings of the 3rd IEEE Conference on Industrial Electronics and Applications.

Yamaguchi, T., and S. Hashimoto, (2009). “Fast crack detection method for large size concrete surface images using percolation based image processing” Machine Vision and Applications 21, (5), 797-809.